Land take futures under divergent urban growth scenarios: Cellular automata-based stress-testing for No Net Land Take targets

Anasua Chakraborty[1], Ahmed Mustafa[2], Lien Poelmans[3], Jacques Teller[1]

[1]LEMA, Université de Liège, Belgium

[2]The New School, New York, USA

[3]Environmental Modelling Unit, Flemish Institute for Technological Research, Belgium

Corresponding author: A. Chakraborty, A.chakraborty@uliege.be

---

This is a non-peer-reviewed preprint submitted to EarthArXiv.

Abstract

Land take, the conversion of greenfield land into built-up areas, poses critical planning challenges for sustainable urban development, particularly as the EU Soil Strategy 2030 sets No Net Land Take (NNLT) by 2050 as a long-term objective for member states across Europe. Addressing this issue requires understanding the balance between outward urban expansion and inward urban densification. This study employs a Multinomial Logistic Regression-based Cellular Automata (MNL-CA) model to simulate two future scenarios of urban development until 2050 in Wallonia, Belgium, a region where, despite planning interventions promoting densification, land take rates remain persistently high, challenging conventional Business-As-Usual (BAU) projections. The model simulates two contrasting built-up demand scenarios. BAU follows a linear extrapolation of historical trends, representing a gradual slowdown of urban expansion and shift to densification. The second, Growth-As-Usual (GAU), applies a stress-test where urban expansion continues steadily through 2050. Under BAU, expansion rates decrease, stabilising at approximately 0 hectares per day by 2040, with total built-up area growing by 8,861 hectares (2.87%) by 2050, reflecting a progressive shift toward compact forms. By contrast, GAU produces ongoing expansion at 2.51 hectares per day in 2050, adding 27,347 hectares (8.87%) of built-up area, highlighting the risks of uncontrolled land consumption. Spatial metrics demonstrate that BAU fosters compact and contiguous development, whereas GAU results in fragmented urban forms that challenge the resilience of spatial planning policies. By evaluating both scenarios, our model provides a framework for stress-testing development strategies, enabling more robust assessments for regional NNLT commitments and sustainable land-use policy.

Keywords: No Net Land Take ; Scenario Modelling ; Cellular Automata ; Urban Densification ; Spatial Planning

1 Introduction

The EU Soil Strategy 2030 sets No Net Land Take (NNLT) by 2050 as a long-term planning objective for member states, recognising that the continued conversion of greenfield land into built-up areas poses a fundamental threat to soil resources, biodiversity, and food security (European Commission (2021)). Yet across Europe, land take continues, driven by two competing processes: outward urban expansion, which converts natural and agricultural land into built environments, and inward urban densification, which intensifies land use within existing urban areas (Seto et al. (2011), Al-Ahmadi et al. (2009), Esposito et al. (2018)). These processes do not operate uniformly: their balance varies across regions in response to distinct environmental, economic, and regulatory conditions (Barros and Balsas (2020), Dewan and Yamaguchi (2009)). Understanding which process dominates – and under what planning assumptions – is therefore central to assessing whether NNLT targets are achievable.

Expansion dominates in developing regions like Sub-Saharan Africa and South Asia, driven by rapid population growth and weak regulatory enforcement, while European cities – constrained by land availability and stronger sustainability mandates – tend to emphasise densification, as seen in Berlin, Paris, and London (Esposito et al. (2018), Kasanko et al. (2006)). Fast-growing centres such as Lagos, Karachi, and Dhaka show both processes occurring simultaneously, complicating planning strategies (Wang and Kintrea (2021), Ullah and Ibrar (2022)).

Urban growth modelling typically relies on the Business-As-Usual (BAU) scenario, which assumes that urban expansion will slow over time due to planning interventions and natural saturation (Thorne et al. (2013)). BAU is particularly relevant for developed cities where compact growth strategies and zoning policies promote densification over uncontrolled sprawl. Nonetheless, this assumption does not hold universally: in regions where land demand remains persistently high, urban expansion continues despite planning efforts, making BAU an overly optimistic projection.

To address this limitation, we introduce the Growth-As-Usual (GAU) scenario, which assumes a continuous or unconstrained urban expansion at a constant rate, without the gradual decline as observed in BAU. GAU serves as a stress-test, evaluating whether current land-use policies and zoning regulations can withstand persistent development pressures (Thorne et al. (2013), Charliers Julien and Reginster Isabelle (2024)). While BAU considers a controlled, policy-driven transition toward densification, GAU provides a worst-case scenario, testing the resilience of urban planning strategies in areas experiencing relentless suburbanization. Unlike previous studies, which often assume urban expansion will eventually stabilise, GAU explicitly models the consequences of unchecked land consumption, offering a critical perspective for urban policymakers.

These growth scenarios are simulated using a Multinomial Logistic Regression (MNL) based Cellular Automata (CA) model. CA is a widely used spatial modelling approach where urban landscapes are represented as dynamic grids of evolving cells, influenced by socio-economic, geophysical, and accessibility factors (Batty (1997), Vermeiren et al. (2012), Mustafa et al. (2018b)). Unlike traditional CA models that rely on simplistic binary expansion patterns, MNL-CA distinguishes between multiple urban density levels (White and Engelen (1997)). Most existing CA-based urban growth models either focus on policy-driven interventions (Liu et al. (2019))

or fail to integrate stress-test scenarios. For instance, Vermeiren et al. (2012) applied logistic regression to predict BAU urban expansion but did not consider dynamic neighbourhood effects. Similarly, Naikoo et al. (2023) modelled probabilistic urban zones but did not explicitly define GAU or stress-test urban policies. In contrast, our study is the first to formally operationalise urban stress-testing within an MNL-CA framework, combining BAU and GAU as complementary scenarios to quantify the planning risk of persistent land consumption in a European transitional-growth region – a replicable approach for assessing whether regional development trajectories are consistent with NNLT objectives.

Wallonia (Belgium) presents an ideal case study for stress-testing NNLT scenarios due to its unique and persistent urbanisation patterns. Since the mid-20th century, the region has experienced rapid suburban expansion, largely driven by transportation network development and housing demand (ESPON (2020)). Despite planning interventions aimed at promoting densification, Wallonia continues to exhibit high land consumption rates. Unlike other European regions where growth has stabilised, it remains in a transitional phase, with both expansion and densification still shaping its urban landscape – challenging BAU's assumptions and making GAU essential for stress-testing the region's spatial planning strategies (Chakraborty et al. (2023)). By applying both scenarios to Wallonia, we quantify the gap between a controlled trajectory and an unchecked expansion trajectory, providing a direct measure of the planning effort required to keep the region on course for NNLT by 2050.

This study focuses on developing an MNL-CA model to simulate urban growth based on the following methodological approach:

- Estimating urban built-up demand based on historical trends derived from existing built-up density maps.
- Developing an MNL-CA model to project future urban expansion and densification.
- Simulating urban built-up expansion under both BAU and GAU scenarios until 2050.
- Establishing a baseline stress-testing framework for evaluating regional land-use trajectories against NNLT targets.

The article proceeds as follows: section 2 describes the study area, datasets, and methods; section 3 presents the simulation under both growth scenarios; section 4 discusses their implications for existing and future urbanisation; and section 5 synthesises policy implications for regional NNLT commitments and directions for further research.

2 Materials & Methodology

The methodology is structured around four components: the study area and datasets that form the model inputs, the MNL-CA workflow used to simulate future scenarios, and the spatial metrics applied to interpret growth patterns, as illustrated in Figure 1.

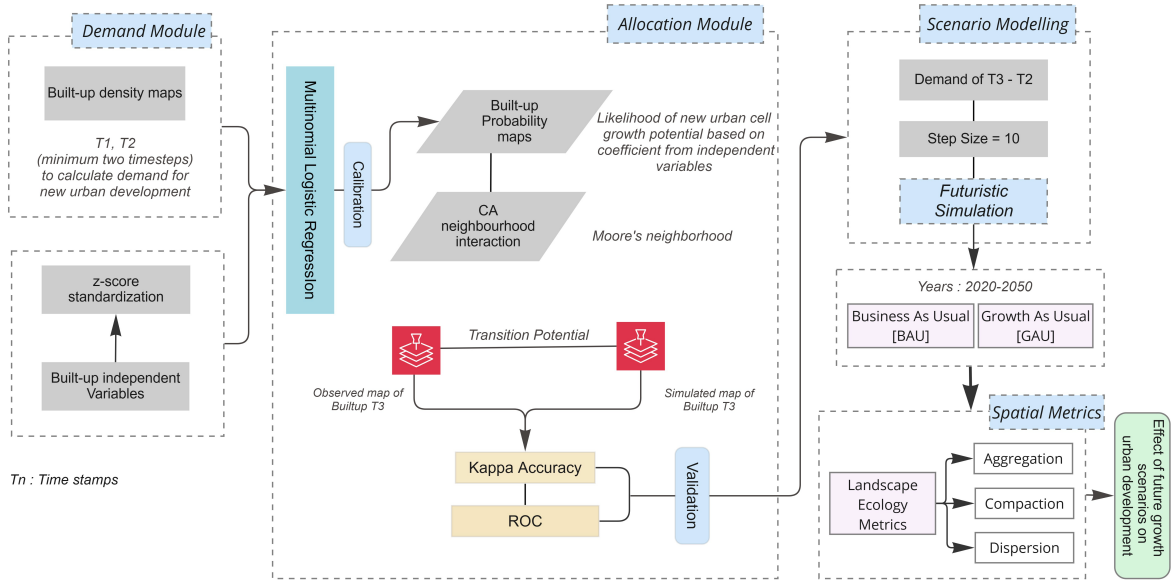


Figure 1: Workflow schema illustrating the MNL-CA modelling process for simulating BAU and GAU urban growth scenarios.

2.1 Study Area

Wallonia – the southern region of Belgium, covering an area of 16844 km^2, is selected as our area of study, with intriguing urban-rural conurbations (Figure 2). Wallonia is one of the most densely populated regions in Europe, with 213 inhabitants/km^2. Due to this growing population and housing demand, the region has experienced high land take since the 1950s. The development of transportation networks has enabled people to settle outside the centre, leading to significant urban expansion. This led to the gradual artificialization of areas predominantly by residential uses, at the cost of agricultural lands. As per the report from 2017 (SPW (2017)), artificialization accounts for 1756 km^2, i.e. 10.4% of the total Wallonia territory.

The post-war economic boom and rising household income encouraged suburbanization. Historically, spatial planning in Wallonia relied on rigid zoning laws and hierarchical sector plans (Hanocq (2011)). The policies (ESPON (2020)) aimed to regulate land use but struggled to keep up with rapid urban growth, leading to fragmented development and inefficient land use. Over time, more strategic and flexible planning strategies were adapted to balance urban expansion with environmental preservation (CPDT (2024)). Despite these efforts, local governance remains crucial: municipalities retain significant power over development decisions, and this decentralised system (Chakraborty et al. (2025)) has created spatial disparities in urban expansion rates across the region.

2.2 Datasets

Our methodology, shown in Figure 1, is designed around the available data. Following Chakraborty et al. (2022a) and Chakraborty et al. (2023), cadastral Data from the Belgian Land registry has been used as the dependent variable for mapping the urban built-up in Wallonia. We have used the attribute of 'construction year' to create Built-up rasters for the years 2000, 2010, and

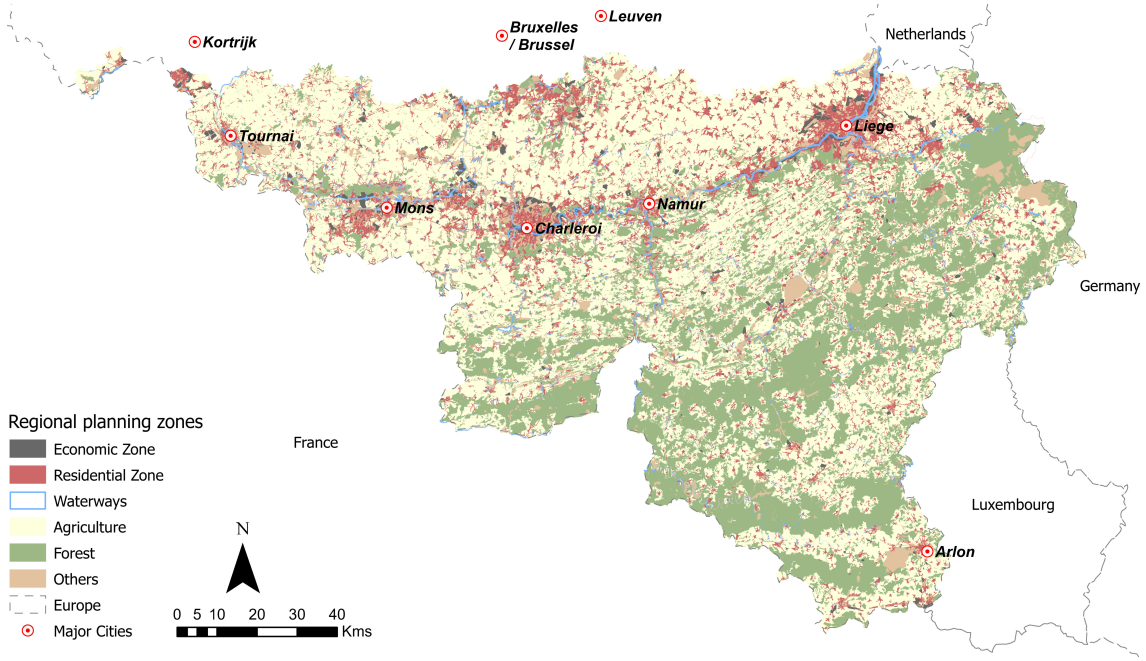


Figure 2: Sector plan of Wallonia showing land use zones and the study area boundary. Map lines delineate study areas and do not necessarily depict accepted national boundaries.

Source: Public service of Wallonia (2020)

2020 at a scale of 100m × 100m corresponding to 1 hectare (ha). This is a commonly used scale for urban modelling studies like Mustafa et al. (2018a) and Chakraborty et al. (2024a). Binary urban growth measures fail to capture the full range of built-up development at a regional scale (Cammerer et al. (2013)); we therefore tested our dependent variable under different levels of density (Chakraborty et al. (2025)). Initially, the cadastral data were rasterised to a 2m × 2m (high resolution) image, but due to heavy computational requirements, we aggregated them to 100m × 100m. We further classified the rasters into four built-up density classes using geometric classification techniques (Mustafa et al. (2018c)). The four density levels include *class 0–Non* built-up, *class 1–Low-density* built-up, *class 2–Medium-density* built-up, and *class 3–High-density* built-up. This follows the dataset-construction method of Chakraborty et al. (2022a) and Chakraborty et al. (2024b). These maps are used for calculating land demand rates of historical built-up which are then used for simulating urban growth for the years 2030, 2040 and 2050.

We selected a list of *twelve* independent variables comprising geophysical, accessibility, and socio-economic factors as shown in Table 1. These variables are known to influence urban growth dynamics (Mustafa et al. (2018a), Mustafa et al. (2018c), Mustafa et al. (2018d)). We have used the Open Street Maps (OSM) (OpenStreetMap Foundation contributors (2024)) to define road type using the data attributes and calculated the Euclidean distance from them. The road types *Motorways* and *Highways* are defined as Road 1. Similarly, roads 2, 3, and 4 represent primary roads, secondary roads, and residential roads, respectively. Similarly, we acquired railway stations as point data from OSM. The slope has been calculated from the

Table 1: List of independent variables used for modelling urban growth scenarios.

Name	Abbreviation	Initial Data Type	Final Data Type	Unit
Elevation	DEM	Raster	Raster	meter (m)
Slope	SL	Raster	Raster	percent (%)
Distance to Road 1	ER1	Vector [a]	Raster	meter (m)
Distance to Road 2	ER2	Vector [a]	Raster	meter (m)
Distance to Road 3	ER3	Vector [a]	Raster	meter (m)
Distance to Road 4	ER4	Vector [a]	Raster	meter (m)
Distance to Railway Stations	ERS	Vector [b]	Raster	meter (m)
Distance to Large Sized Cities	ELC	Vector [b]	Raster	meter (m)
Distance to Medium Sized Cities	EMC	Vector [b]	Raster	meter (m)
Employment Density	EMD	Vector [c]	Raster	per inh
Population	POP	Vector [c]	Raster	numeric
Zoning	ZON	Vector [c]	Raster	meter (m)

Vector data type that has been used for pre-processing: [a]Line, [b]Point, [c]Polygon
All the data have been resampled to 100m × 100m and standardized before running the modelled scenarios

Digital Elevation Model derived from the Geoportal website of Wallonia by Public service of Wallonia (2020). The total population and the number of jobs, represented as the employment rate, have been considered socio-economic variables. While the former was derived at the statistical sector level, the latter was calculated at the municipal level, based on data from the Belgian statistical office (Statbel, Statbel (2017)). One of the most important variables in our study is zoning, shown to play a crucial role in urban development processes in Belgium (Poelmans and Van Rompaey (2010), Mustafa et al. (2018d), Chakraborty et al. (2022a)). Belgium's sector plan or *Plan de secteur*, as called in Wallonia, provides information about zones and their designated uses (Figure 2). Hence, we created a binary zoning map where 0 means cells that are not permitted for urban development and 1 means permitted for further development.

Prior to modelling, independent variables were standardised using z-score normalisation and screened for collinearity using the Variance Inflation Factor (VIF), retaining only variables with VIF < 4, similar to C. Montgomery et al. (2012).

2.3 Demand calculation

We model the future urban growth scenarios by extrapolating their past demand under two different demand conditions. *Demand* refers to the development of new built-up cells observed between two time-stamps *T1* and *T2* as shown in Figure 1. While this demand can be expressed per day or per year, our study performs a long-term assessment considering two decades: 2000–2010 and 2010–2020, to simulate future growth until 2050. Our study uniquely considers the built-up demand as a combined phenomenon – we differentiate between the outward expansion and densification in areas with existing built-up.

As noted in section 1, we use the class-to-class transition matrix for urban built-up (2000–2010 and 2010–2020) to calculate demand for subsequent years and model built-up change under BAU and GAU. The transitions from reference class 0 to classes 1, 2, and 3 are considered as urban expansion, and transitions from class 1 to 2 and 3, and class 2 to 3, are considered urban

densification. The full transition matrix is provided in Table S1 of the supplementary material.

The demand simulation in the case of BAU is calculated according to Equation 1. It is the mathematical formulation for extrapolating demand for any particular class transition, for the BAU scenario. This is accomplished using the demand data of two previous years.

$$d = \frac{D_n - D_m}{n - m}, \quad n > m \tag{1a}$$

$$D_x = D_n + (x - n) \times d, \quad \text{where} \quad x \in \mathbb{Z},\ D_x \geq 0 \tag{1b}$$

where D_x is the yearly demand at year x and d is the change rate used to extrapolate the demand for the simulation.

Equation 1a calculates the change in demand between two years m and n, over the duration $n - m$ years. Demand at any year x is assumed to be constant throughout that particular year. For the subsequent year, the demand is recalculated. Thus, we obtain the yearly "rate" of change d, assuming that the change is linear. Equation 1b explains how this change rate d can then be used to extrapolate over the following years to predict 2030, 2040 and 2050. This yearly demand, hence calculated, is used for modelling the allocation of class transitions.

A worked numerical example applying Equation 1 to the class 0-to-1 transition – illustrating the declining BAU rate against the constant GAU rate – is provided in the supplementary material.

2.4 Cellular Automata modelling for scenario simulation

In this study, we use CA modelling (Batty (1997), Li and Yeh (2000)), valued for its dynamic, temporally explicit nature, to allocate the demand (as explained in subsection 2.3) for future urban expansion and densification under BAU and GAU scenarios in 2030, 2040 and 2050.

The transition rule is defined based on two components :

- Probability maps derived by Multinomial Logistic regression (MNL) model.
- Neighbourhood calibration using CA Model.

2.4.1 Model Calibration and Probability Maps

Clarke et al. (1996) elucidates the importance of calibration in modelling for near-realistic simulation. In this study, we employ an MNL to calibrate our dependent variable (e.g. built-up changes) based on various independent variables as shown in Table 1. It analyses changes for class 0 (no-change/transition to class 1, 2, or 3), class 1 (no-change/transition to class 2), and class 2 (no-change/transition to class 3). Similar to the studies by Mustafa et al. (2018b) and Chakraborty et al. (2022b), we divided our data into a 70–30 ratio of training and testing sets. The training set comprises 24034 randomly sampled cells (the 70%), ensuring minimal autocorrelation for the years 2000–2010. This is an efficient way to handle autocorrelation (Overmars et al. (2003)) in our dependent variables, i.e., urban built-up maps (Cammerer et al. (2013)).

The probability maps are obtained for each class by fitting an MNL model on the independent variables in Table 1; the full equation is provided in the supplementary material.

The MNL model provides coefficients that compute probability maps for new urban cell growth and reveal each variable's positive or negative impact. We also computed the significant independent variables with $p\text{-}value < 0.01$. These maps are then used as input for defining transition rules and spatial allocation of future urban growth demand.

2.4.2 Neighbourhood effect on demand allocation

The probability alone does not consider the local effect of urban built-up. Hence, we use the CA model to calibrate the neighbourhood effect on urban growth. To do so, we use a 3 × 3 grid of cells – also known as Moore's neighbourhood. This particular window size has been chosen as multiple studies (White and Engelen (2000), Poelmans and Van Rompaey (2009)) have proved it to be efficiently capturing urban growth phenomena because of its easy configuration and sufficient local characteristics (Zhang and Wang (2021)). Additionally, we have conducted a global sensitivity analysis to choose the best parameters and neighbourhood combination, and concluded that a 3 × 3 neighbourhood size is well-suited for simulating urban growth scenarios in the region of Wallonia (Chakraborty et al. (2025)). The neighbourhood of a given cell is computed as follows.

$$N_{ij}^{c_1,c_2} = \sum_{n=j-1}^{j+1} \sum_{m=i-1}^{i+1} \delta(c_{mn}, c_2) \cdot (1 - \delta_{m,i} \cdot \delta_{n,j}) \tag{2a}$$

$$\text{where} \quad \delta_{a,b} = \begin{cases} 1, \text{ if } a = b, \\ 0, \text{ otherwise.} \end{cases} \tag{2b}$$

where $N_{ij}^{c_1,c_2}$ is the 3 × 3 Moore's neighbourhood for the cell at index (i, j). The cell is to transition from class c_1 to class c_2. Here, $N_{ij}^{c_1,c_2}$ is defined as the number of cells in the neighbourhood of cell (i, j) that have the class c_2. Equation 2a calculates the neighbourhood by comparing the class of each cell in the neighbourhood (c_{mn}) with c_2. $\delta_{a,b}$ here is the Kronecker delta function, defined in Equation 2b.

Consolidating the effects of both – the probability maps from MNL $(P_{ij}^{c_1,c_2})$ and the neighbourhood interactions $(N_{ij}^{c_1,c_2})$ as described above, we define the transition potential $(T_{ij}^{c_1,c_2})$ – the realistic likelihood of a cell (i, j) transitioning from class c_1 to c_2, below, in Equation 3a. Following this, we form the transition rule, which is a mathematical formulation for the spatial allocation of the potent cells at every time step. It makes the backbone of our MNL-CA model. To incorporate a degree of randomness while preserving the transition potential as the primary determinant, transitions are permitted only when their potential exceeds a randomly generated value drawn from a Gaussian distribution constrained between 0 and 1 (Equation 3b).

$$T_{ij}^{c_1,c_2} = \sqrt{P_{ij}^{c_1,c_2} \times N_{ij}^{c_1,c_2}} \tag{3a}$$

$$T_{ij}^{c_1,c_2} > n, \quad n \in U([0, 1]) \tag{3b}$$

Using this transition rule, we cumulatively allocate new built-up cells each year (time step

T_n) to build the simulated map, first simulating 2020 (from 2000–2010 demand) to compare against the observed map for that year.

2.4.3 Validation of the Model

Once we simulate the map for 2020, we validated it with the observed 2020 urban built-up maps before further simulation. We used two well-known metrics to validate the model's output:

1. **The Relative Operating Characteristics (ROC)** curve evaluates the goodness of fit in MNL models by comparing a probability map with actual outcomes (Hu and Lo (2007)). The key component of ROC analysis is the Area Under the Curve (AUC), which measures the model's ability to distinguish between classes, with values ranging from 1.0 (perfect) to 0.5 (no discriminative power) (Pontius and Schneider (2001)). ROC is particularly suited to urban growth validation as it is independent of class distribution, allowing fair comparisons across density transitions (Chen et al. (2014)). AUC is computed from the trade-off between the True Positive Rate and False Positive Rate; the formal definitions are provided in the supplementary material.

2. **Kappa Statistics (Cohen's Kappa, κ)** assesses the agreement between two categorical variables in classification tasks. In urban growth modelling, κ compares predicted and observed land cover to evaluate model accuracy (Congalton (1991)). Unlike ROC, κ values range from -1 to 1, where 1 indicates perfect agreement, 0 represents random chance, and negative values suggest less agreement than expected by chance (Rwanga et al. (2017)). κ accounts for chance agreement in a way simple accuracy does not, making it a widely used measure in urban growth and land-use change models (Li and Yeh (2000)); the general formula is provided in the supplementary material.

With validation confirmed, we simulate future predictions for 2030, 2040 and 2050 under BAU and GAU to evaluate spatial land-take distribution.

2.5 Spatial metrics as a measure of land-take

Spatial metrics extend the quantitative analysis of land take beyond total area consumed, capturing the spatial structure and fragmentation patterns that distinguish BAU from GAU outcomes. Hence, we developed a Python workflow to compute spatial metrics determining the kind of urban growth primarily governing the land-take in our study area for both the growth scenarios.

Wallonia has a dominance in rural development with some important urban cores like Liege, Mons, Namur, etc. (Figure 2). While most studies deal with the amount of land-take or area consumed by urban growth, there are few works done for understanding the spatial pattern governing them (Colsaet et al. (2018)). Below, in Table 2, are the selected spatial metrics used in our study to understand the landscape pattern under growth scenarios.

Table 2: Description of selected metrics used in urban growth analysis.

Metric	Formula	Explanation
Urban Sprawl Index (USI)	$USI = \frac{\text{Built-up area}}{\text{Urban extent}}$	Measures the extent of sprawl by assessing the ratio of built-up area to urban extent.
Shannon Entropy (SE)	$H = -\sum_{i=1}^{n} p_i \ln(p_i)$	Quantifies urban distribution uniformity; higher values indicate more dispersed growth.
Patch Density (PD)	$PD = \frac{\text{Number of patches}}{\text{Total area}}$	Describes fragmentation; higher values signify more fragmented urban landscapes.
Average Contiguity (AC)	$AC = \frac{\sum \text{Contiguity of patches}}{\text{Number of patches}}$	Indicates urban compactness; higher values suggest more contiguous growth.

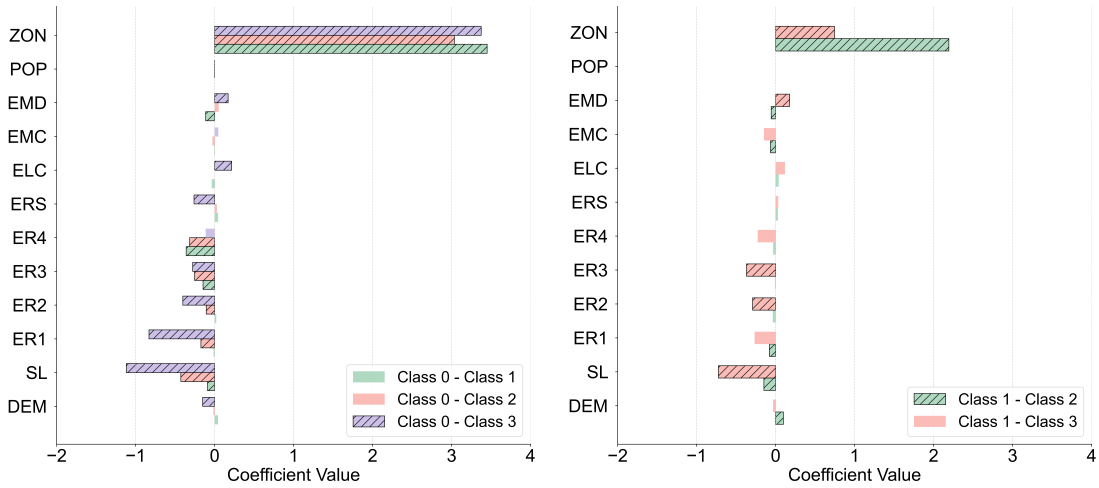
3 Results

3.1 Impact of independent variables on urban growth

We calibrated our MNL model for urban expansion (class 0 to 1, 2, and 3) and densification (class 1 to 2/3, class 2 to 3), producing coefficients for each variable's contribution to these processes.

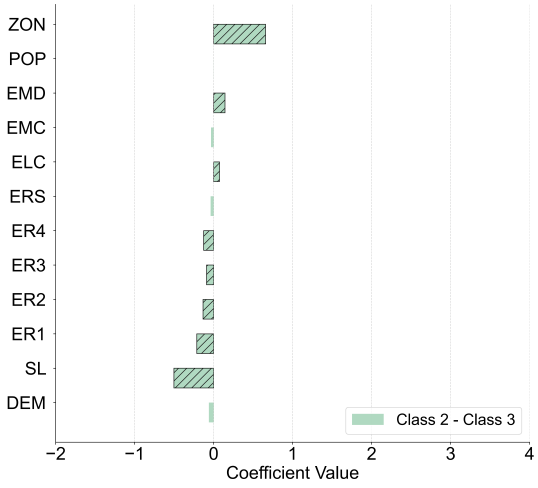
Our findings, depicted in Figure 3, show that Zoning (ZON) policies emerge as the most significant independent variable exhibiting a positive impact on the **urban expansion** process with coefficient values of 3.450, 3.035 and 3.374. This observation is in line with Mustafa et al. (2018b) and Poelmans and Van Rompaey (2010). As for the geophysical factors, Elevation (DEM) has an overall positive impact on the development of low-density cells (coefficient of 0.042) while having a negative impact on high-density built-up development. Slope (SL), on the other hand, has a negative impact across all three built-up classes. Overall, we observe that distance to roadways, particularly Highways ($ER1$), has a negative impact on the urban expansion processes. Distance to railway stations (ERS) has no significant impact on low and medium built-up density and a negative impact on high-density expansion, i.e. cells located further away from the stations have a lower chance of being urbanised with high-density cells. Distances to large and medium cities (ELC and EMC respectively) have a positive impact with values 0.001 and 0.216, on high-density expansion. On the contrary, both have a negative impact, particularly in low-density expansion. Employment density (EMD) has a positive impact on higher-density built-up, while it reflects a negative, but significant, impact in low-density built-up expansion.

While calibrating **urban densification** using MNL, zoning again emerges as a significant positive driver, akin to expansion. Elevation derived from DEM and slope largely affect the process with an increase in density levels. However, the negative coefficient has significance in terms of its p-value. The densification process is also negatively impacted by distance to *roads*, though significance prevails only in medium and high built-up classes. Similar to expansion, ERS (Table 1) reflects a positive coefficient of 0.027 and 0.031 (class 1 to 2 and 3), and a negative coefficient in medium to high-density class transition. However, the impact of railway stations does not show a significant relationship. Distance to Large cities holds a non-significant



(a) Urban expansion (reference class 0)

(b) Densification from class 1



(c) Densification from class 2

Figure 3: Bar charts showing MNL coefficients for different transitions.
(*Hatched bars indicate variables significant at p-value* < 0.01.)

impact on medium and high-density built-up areas, while medium cities negatively impact urban densification. The density of jobs attracts more built-up development, with significant positive coefficients (0.177 and 0.144) for medium and high-density built-up, respectively.

The MNL model's calibration was evaluated using probability maps of built-up occurrence compared against the observed binary map, with values > 0.5 indicating a good fit (Hu and Lo (2007)). We computed the ROC for urban expansion (class 0 to 1, 2 and 3): 0.790, 0.840, and 0.930 for classes 1, 2 and 3, respectively. Similarly, ROC for densification ranged from 0.978 to 0.991 across class transitions, also suggesting high calibration ability of MNL (full transition matrix in Table S3 of the supplementary material).

3.2 Accuracy assessment for MNL-CA growth modelling

We simulated the built-up map for 2020 from 2000–2010 demand data and compared it with the observed 2020 built-up map, derived from Belgium's cadastral data, to assess the model's

predictive accuracy.

The model achieved high ROC values across built-up density classes: 0.994 (class 0), 0.923 (class 1), 0.963 (class 2), and 0.965 (class 3). The overall Cohen's Kappa (κ) coefficient was 0.925, indicating substantial agreement between the observed and simulated maps. Figure S1 of the supplementary material shows the built-up map for Liège and its surroundings alongside a pixel-level accuracy map comparing the observed and simulated built-up for 2020, highlighting areas of alignment with observed data as well as regions with notable discrepancies.

The calibration accuracy of a model typically surpasses its validation accuracy (Al-Ahmadi et al. (2009)). This limitation can be attributed to the simulation's inability to account for the inherent uncertainty in the allocation of built-up areas observed in real-world scenarios. To address this, we incorporated a stochastic component into the CA model, which improved its ability to handle variability and achieve realistic simulations.

3.3 Simulation of future urban development under the BAU and GAU scenarios

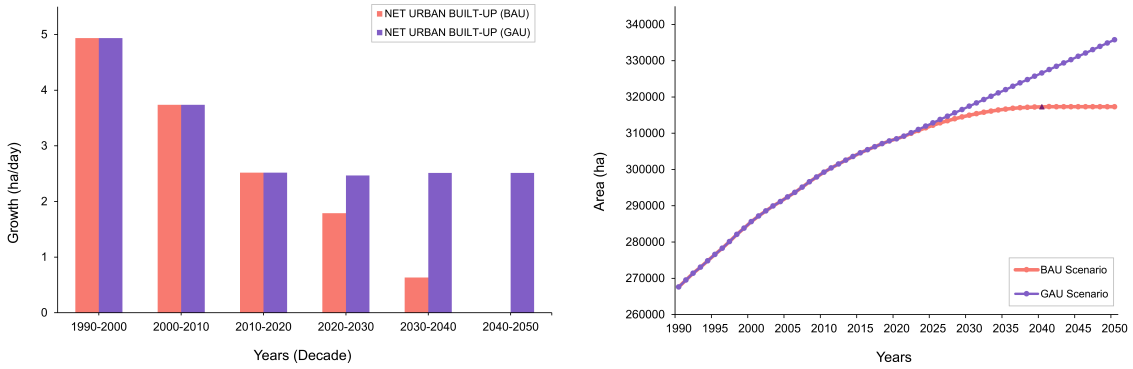
Using the MNL-CA model, we allocated demand for both scenarios to analyse temporal changes in urban growth through 2050. Previous studies, such as Mustafa et al. (2018a) and Thorne et al. (2013), have employed *BAU* growth approaches for future scenarios, by linearly extrapolating the past demand over multiple years to simulate future scenarios. Similar to their findings, we identified a progressive shift from expansion to densification in Wallonia between 2000–2020 (Table S1, supplementary material).

The BAU scenario, which extrapolates historical demand, shows a steady decrease in land take over time. Starting at 1.79 hectares/day in 2020, the daily land take gradually reduces to 0 hectares/day by 2040 itself, indicating a complete stabilisation in demand for new urban land. This stabilisation serves as an *inflection point* for expansion demand and is reflected in Figure 4(a), where the BAU curve flattens after 2040. Our study reveals a decline in demand for expansion (from class 0 to classes 1, 2, and 3) and a corresponding rise in demand for densification, aligning with these trends. The total built-up area under BAU increases by 8,861 hectares between 2020 and 2050, corresponding to a growth of 2.87%. In contrast, the GAU scenario assumes a constant land take rate of 2.51 hectares/day throughout the simulation period, leading to a significantly higher cumulative increase in built-up area. By 2050, the GAU scenario adds 27,347 hectares, resulting in a total growth of 8.87%.

The net built-up area over time (Figure 4(b)) mirrors these trends: BAU tapers and stabilises by 2040, while GAU maintains a consistent positive slope through 2050.

In the BAU scenario, the rate of decline in the demand for expansion exceeds that of densification, leading to higher expansion until 2020, after which densification becomes the prevailing trend. The decade-by-decade demand underlying these trends is provided in Table S4 of the supplementary material.

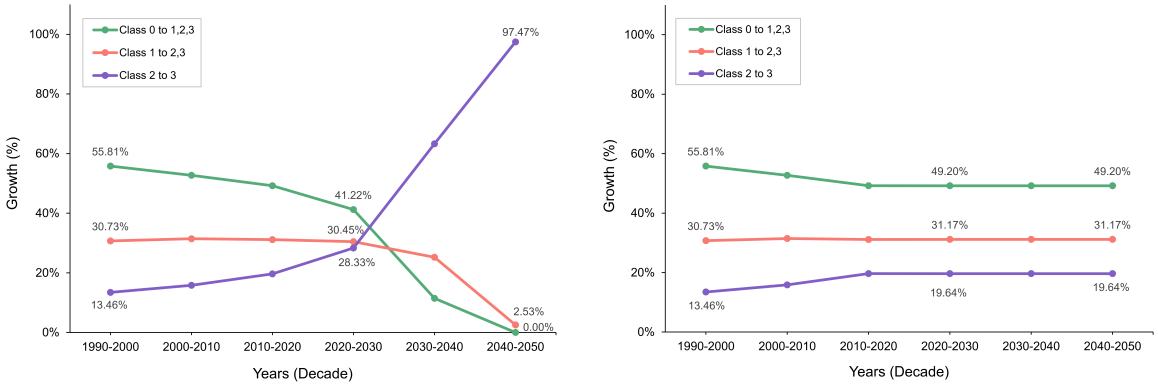
Figure 5 shows the class-wise divergence: BAU's demand for outward expansion declines notably over time, while GAU sustains a steady share. This divergence is evident in class 1 (low-density urban land), which consistently declines, shrinking by 2,286 hectares (-2.94%) under BAU and 3,166 hectares (-4.08%) under GAU. Meanwhile, class 2 (medium-density urban



(a) Plot of simulated demand, depicting the divergence in the BAU and GAU scenarios.

(b) Plot of area occupied by urban land, as a function of time.

Figure 4: Simulated land take and built-up area trajectories under BAU and GAU scenarios from 2020 to 2050.



(a) BAU scenario: expansion declines sharply, with densification becoming dominant by 2040.

(b) GAU scenario: expansion and densification rates remain stable through 2050.

Figure 5: Decade-wise percentage of expansion and densification under BAU and GAU scenarios from 1990 to 2050.

land) grows modestly by 1,271 hectares (+0.76%) under BAU but expands substantially by 16,590 hectares (+9.87%) under GAU, highlighting its increasing role in urban growth. Class 3 (high-density urban land) shows changes, with a 15.75% increase under BAU and a 22.20% rise under GAU. These class-wise changes are summarised in Table S5 of the supplementary material.

Table 3 presents the quantified changes in spatial metrics across scenarios and years, highlighting distinct urban growth patterns. The Urban Sprawl Index (USI) increases from 0.658 in 2020 to 0.668 under the BAU scenario and 0.697 under the GAU scenario by 2050, indicating a higher degree of sprawl in the GAU scenario. Similarly, *Shannon Entropy* (SE) rises from 0.950 in 2020 to 0.957 under BAU and 0.976 under GAU, reflecting greater spatial heterogeneity under the latter. Class-wise Average Contiguity (AC) shows a notable increase, particularly in classes 2 and 3, with values reaching 3.936 and 5.248 under BAU and 5.760 and 5.810 under GAU, by 2050. Patch Density (PD) decreases over time for all classes, with lower values observed in GAU compared to BAU in 2050, indicating fewer but larger urban patches in the former.

Table 3: Table showing selected urban growth parameters for different scenarios and years.

Year	Scenario	USI	SE	Class	AC	PD
2020	-	0.658	0.950	Class 0	382.987	1.81E-07
				Class 1	0.398	1.50E-06
				Class 2	3.394	1.16E-06
				Class 3	3.485	4.64E-07
2050	BAU	0.668	0.957	Class 0	538.398	1.29E-07
				Class 1	0.472	1.40E-06
				Class 2	3.936	1.05E-06
				Class 3	5.248	4.18E-07
2050	GAU	0.697	0.976	Class 0	632.839	1.08E-07
				Class 1	0.684	1.22E-06
				Class 2	5.760	9.01E-07
				Class 3	5.810	4.17E-07

Choropleth maps show the spatio-temporal distribution of built-up density across 262 municipalities in Wallonia (Figure 6), using a geometric interval classification that divides values into five ranges, with darker colours indicating higher values (Figure 7 and Figure 8); the corresponding total built-up area per municipality is provided in Figures S2 and S3 of the supplementary material.

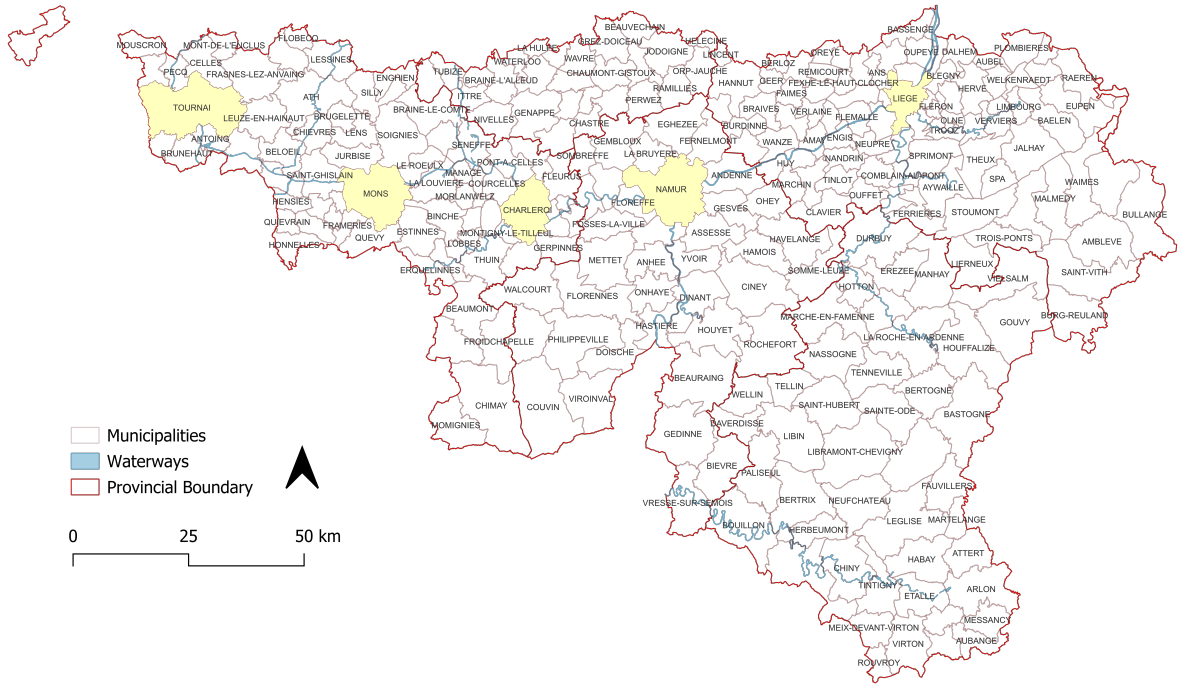


Figure 6: Administrative boundaries of the municipalities of Wallonia used as spatial units for choropleth mapping of built-up density change. Map lines delineate study areas and do not necessarily depict accepted national boundaries.

Under the BAU scenario (Figure 7), urban expansion from class 0 to 1, 2, and 3 remains limited, with growth concentrated primarily in urban centres (Figure 2) and their nearby suburban areas during the 2020–2030 period. Expansion diminishes significantly by 2040–2050, though areas surrounding the main urban centres continue to expand, albeit at a slower pace. Densification, characterised by transitions from class 1 to class 2 and subsequently to class 3, is predominantly confined to urban cores, with minimal transformation occurring in rural and less urbanised municipalities in southern Wallonia. Conversely, the GAU scenario (Figure 8) projects more extensive and accelerated land-use changes, marked by geographically dispersed expansion and pronounced densification beyond urban cores. Growth extends into peri-urban and rural areas, with notable intensification occurring in municipalities under population pressures and near economic hubs such as Charleroi, Liège, Namur, and the Brussels periphery (e.g., Wavre and Ottignies-Louvain-la-Neuve). These contrasting trajectories and their spatial implications are examined in the following section in the context of Wallonia's land-use planning challenges and NNLT commitments.

4 Discussion

4.1 Model performance and drivers of urban growth

The MNL model's high calibration accuracy and validation performance provide a robust foundation for analysing urban transitions under BAU and GAU scenarios. Flat terrain encourages low-density growth while rugged topography hinders it, and together with zoning policy and proximity to employment hubs, these factors emerge as critical drivers of urban densification, consistent with Wallonia's historical and regulatory context. These results depict that Wallonia follows an infrastructure-oriented development similar to (Poelmans and Van Rompaey (2010), Mustafa et al. (2018d), ESPON (2020)). Supporting this, the negative impact of roads and railway stations shows that Belgium does not enforce a transit-oriented development. Despite zoning restrictions, urban expansion in peri-urban areas like Gembloux and Ciney continues due to their strategic location between Brussels and Namur, with commuters seeking affordable housing while maintaining access to employment centres, where major cities and their infrastructure influence the urban growth of their peripheral areas (Figure 7 and Figure 8).

BAU reflects decreasing land consumption, transitioning toward densification, with urban expansion slowing post-2040, as supported by Mustafa et al. (2018c) and Charliers Julien and Reginster Isabelle (2024). While adaptive local governance policies contribute to compact growth, socioeconomic forces (including employment accessibility, commuting patterns, and housing demand) also drive densification. High-accessibility locations like Liège, Namur, and Charleroi attract urban intensification, often independent of zoning policies. In contrast, GAU, with weaker regulatory control, fosters suburban sprawl, particularly in municipalities without strong containment measures.

4.2 Spatial patterns of urban growth under BAU and GAU

Urban growth under the BAU scenario is more controlled and compact than in GAU, as reflected in spatial metrics: a lower *USI* and higher *AC* reflect reduced sprawl and increased densifica-

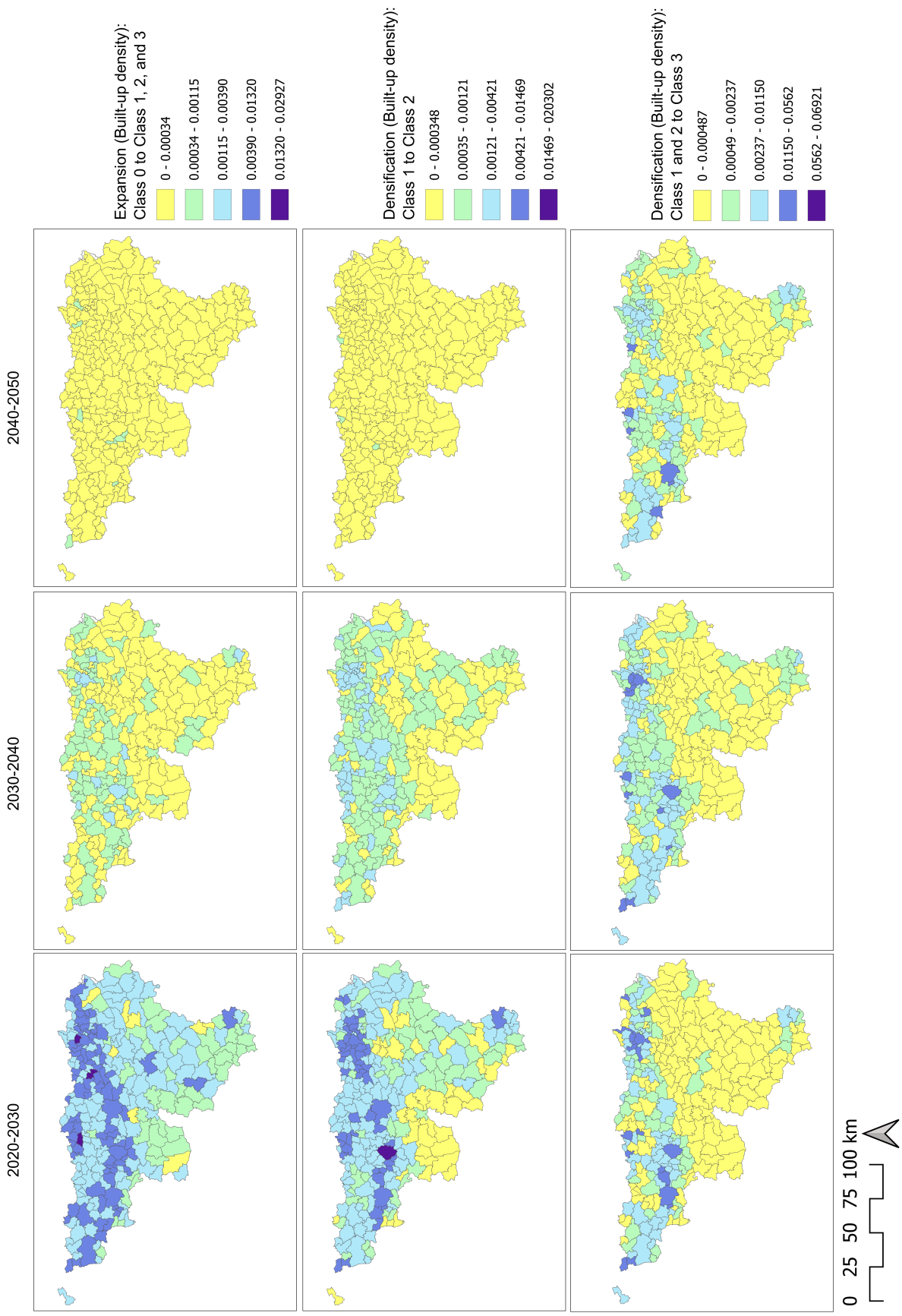


Figure 7: Choropleth maps showing municipality-level built-up density change under the BAU scenario for 2020–2030, 2030–2040 and 2040–2050. Map lines delineate study areas and do not necessarily depict accepted national boundaries.

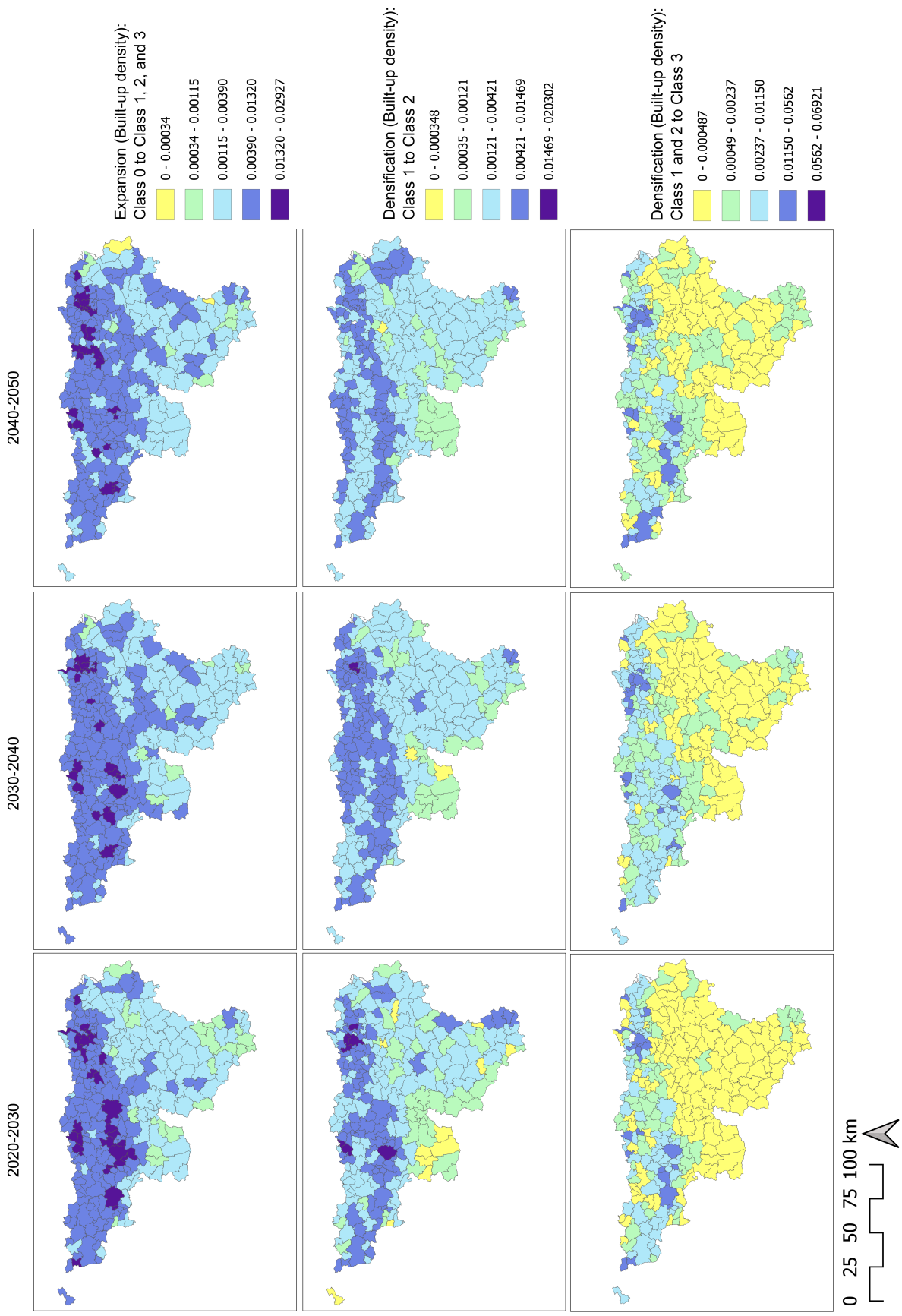


Figure 8: Choropleth maps showing municipality-level built-up density change under the GAU scenario for 2020–2030, 2030–2040 and 2040–2050. Map lines delineate study areas and do not necessarily depict accepted national boundaries.

tion in major municipalities like Liège, Namur, areas near Brussels (e.g., Louvain-la-Neuve) (Figure 6), and peri-urban centres like Mons, La Louvière, Arlon, and Bastogne. Market forces play a key role alongside infill and containment policies: housing demand in well-connected employment hubs drives densification even without strict zoning, as seen in Liège's intensification into a logistics hub, with the *Trilogiport* inland port and Airport attracting large new developments. Consequently, BAU results in fewer but larger, more cohesive, better-connected urban patches (Figure 7 and Figure 8), with Liège and Namur prioritising densification over outward expansion. Exceptions persist, however: a few patches around Liège, Charleroi, and Mons still expand outward, as in conurbation municipalities like Fléron and Ans, and rising property prices in Brussels push residents toward affordable suburbs like Waterloo and Jodoigne, complicating BAU's containment of sprawl. In contrast, GAU fosters fragmentation, with weaker containment measures enabling uncontrolled suburban sprawl in peri-urban and rural municipalities.

The GAU scenario, representing a *laissez-faire* approach of urban growth, is a cautionary view of the potential consequences of uncontrolled urban expansion. Spatial metrics under GAU reveal higher levels of urban sprawl, with municipalities like Charleroi, Liège, and the municipalities of Walloon Brabant experiencing a more extensive development, often spilling into rural and peri-urban areas. This pattern of fragmented growth, with lower AC and higher USI, underscores the risks of an expansionist approach to urban development. While expansion is dominant across Wallonia in the case of GAU, densification is more prominent in and around cities and prosperous municipalities of Walloon Brabant, like Wavre, Lasne, Louvain-la-Neuve, etc.

4.3 Implications for No Net Land Take

These contrasting spatial outcomes – illustrating the fundamental tension between a policy-aligned trajectory toward densification and the risks of unchecked expansion – have direct quantitative implications for Wallonia's trajectory toward No Net Land Take. Under BAU, land take – defined as the conversion of non-built-up land to built-up classes – reaches zero by 2040, a full decade before the EU Soil Strategy 2030's NNLT objective deadline of 2050 (European Commission (2021)). The continued growth in total built-up area beyond 2040 under BAU reflects ongoing densification within already-built land, which does not constitute land take and is in fact the intended outcome under NNLT. In this sense, a sustained BAU trajectory does not merely approach NNLT – it achieves it ten years ahead of the target. Under GAU, by contrast, land take continues at 2.51 hectares per day through 2050, adding 27,347 hectares of built-up area – a trajectory that is fundamentally incompatible with NNLT and quantifies, in concrete regional terms, what planning failure looks like at the scale of a single member state region.

However, the critical question is whether BAU is realistic. The BAU scenario extrapolates a declining trend in land take derived from historical data for 2000–2020. This decline is a projection, not a guarantee. Wallonia's own planning history – persistent suburbanisation despite decades of zoning interventions, as documented by Charliers Julien and Reginster Isabelle (2024) – gives reason to question whether the conditions that produced the historical declining trend will continue uninterrupted through 2040. If planning enforcement weakens, if housing

demand intensifies, or if market pressures outpace regulatory capacity, the declining trajectory stalls and the region's land take profile shifts toward GAU. This is precisely the risk that the GAU stress-test is designed to expose. The 18,486-hectare gap between BAU and GAU outcomes is therefore not merely a modelling result – it is a measure of the planning effort required to keep Wallonia on a BAU-consistent path, and of the consequences if that effort falls short.

These findings also connect to Sustainable Development Goal 11, Target 11.3, which calls for inclusive and sustainable urbanisation and enhanced participatory planning by 2030. BAU's declining land take trajectory is more consistent with the land-use efficiency principles underpinning SDG 11, Target 11.3 – measured through the ratio of land consumption rate to population growth rate – than GAU's sustained expansion, which drives land consumption well beyond what population growth alone would justify. At the regional level, Wallonia's own Spatial Development Strategy (SDT, Schéma de Développement du Territoire) promotes densification and the consolidation of urban centralities as its primary spatial planning objectives (CPDT (2024)). The BAU scenario, shaped by historical trends and existing zoning policies, aligns broadly with SDT objectives. The GAU scenario illustrates the consequences of insufficient enforcement of those objectives – persistent suburbanisation overriding planned densification.

4.4 Transferability of the BAU–GAU framework

While this study focuses on Wallonia, the BAU–GAU framework has broader relevance for European regions experiencing similar transitional growth dynamics. Within Belgium itself, Flanders offers an instructive contrast: despite sharing the same federal context, Flanders has developed a more centralised and enforceable spatial planning framework since the 1980s, with stronger instruments for containing peri-urban expansion and redirecting growth toward existing urban cores (Poelmans and Van Rompaey (2009), ESPON (2020)). This suggests that the conditions for sustaining a BAU-consistent trajectory toward NNLT are achievable within the same national context, given sufficient regulatory commitment and governance capacity. The Netherlands presents a more cautionary parallel: despite a long-standing reputation as a planner's paradise with compact city policies dating to the 1950s, the gradual devolution of national spatial planning toward decentralisation produced uneven densification outcomes and continued greenfield development (Claassens et al. (2020)), demonstrating that policy intent alone does not guarantee a BAU trajectory holds. Beyond Belgium, the peri-urban peripheries of large metropolitan areas across Europe, including those around Paris and Brussels, share Wallonia's pattern of persistent suburbanisation driven by housing affordability pressures and commuter demand, where BAU's optimistic assumptions are equally open to question (Kasanko et al. (2006)). In this comparative context, the GAU stress-test is not a Wallonia-specific methodological choice but a transferable planning tool applicable wherever the gap between policy intent and observed land take trends remains wide.

4.5 Limitations

Despite its contributions, this study has several limitations. First, the linear BAU extrapolation (from 2000–2020 data) cannot anticipate non-linear shifts from economic shocks, demographic change, or abrupt policy shifts. Second, the scenarios are purely trend-based rather

than linked to Shared Socioeconomic Pathways (SSPs), limiting comparability with European-scale climate and land-use modelling frameworks. Third, the 100m × 100m resolution captures broad trajectories across 262 municipalities but not fine-grained processes such as plot-level infill or vertical densification, which are increasingly relevant to NNLT-oriented planning. Fourth, the 2000–2020 calibration window reflects a specific period in Wallonia's planning history, and the model's coefficients are sensitive to the regulatory and market conditions that prevailed then. Fifth, the model predates Wallonia's 2019 SDT update, whose densification objectives may shift the planning context beyond what the historical trend captures. Finally, the model omits supply-demand feedback: as land becomes scarcer under BAU, demand may respond in ways not captured here, over- or understating densification. These limitations point to future research directions: SSP-based demand projections, finer-resolution modelling, and dynamic land-demand feedback.

5 Conclusion

This study demonstrates that the choice of demand scenario in urban growth modelling is not merely a technical decision; it is a planning and policy statement. By simulating BAU and GAU trajectories for Wallonia through 2050 using an MNL-CA framework, we show that the gap between a declining land take trend and a sustained one amounts to 18,486 hectares of additional built-up area, a difference that is directly interpretable as the cost of planning failure at the regional scale.

Under BAU, land take reaches zero by 2040, a full decade ahead of the EU Soil Strategy 2030's NNLT objective, with lower *USI*, higher *AC*, and reduced fragmentation reflecting the compact, contiguous urban form that NNLT-consistent planning is designed to produce. This outcome, however, is a projection rather than a guarantee: it depends on the regulatory and market conditions behind the historical decline continuing uninterrupted through 2040, a continuation Wallonia's own history of persistent suburbanisation despite zoning intervention gives reason to question. The GAU scenario quantifies what happens if they do not: 27,347 hectares of additional built-up area, sustained land take of 2.51 hectares per day through 2050, and fragmented sprawl patterns fundamentally incompatible with NNLT. GAU is not a prediction but a stress-test, and the 18,486-hectare gap between scenarios is the planning risk it exposes.

For Wallonia specifically, this gap has direct implications for the Spatial Development Strategy (SDT): its objectives of densification and consolidation of urban centralities are precisely the instruments whose effectiveness will determine whether Wallonia follows a BAU or a GAU trajectory. The findings suggest that without sustained enforcement of SDT objectives, particularly in peri-urban municipalities where market pressures continue to drive suburbanisation beyond policy-driven densification, the region risks drifting toward GAU outcomes despite its formal NNLT commitments.

Beyond Wallonia, the BAU–GAU framework offers a transferable approach for stress-testing regional land-use trajectories against NNLT objectives. Any region where historical demand data are available and where the credibility of BAU projections is uncertain, which describes much of transitional-growth Europe, can apply this dual-scenario approach to quantify planning

risk and evaluate the adequacy of existing policy instruments. The MNL-CA model developed here, with its multi-density class structure and combined treatment of expansion and densification demand, provides a replicable methodological foundation for such assessments. As European regions move toward implementing NNLT commitments under the EU Soil Strategy 2030, frameworks that can translate aspirational targets into quantified regional planning gaps will be essential tools for evidence-based spatial policy.

Authorship contribution

Anasua Chakraborty: writing – original draft, validation, software, resources, methodology, investigation, formal analysis, data curation, conceptualisation. Ahmed Mustafa: writing – review & editing, software, supervision, and conceptualisation. Lien Poelmans: writing – review, methodology, investigation, conceptualisation. Jacques Teller: writing – review & editing, supervision, investigation, funding acquisition.

Declaration of conflicting interests

The authors reported no potential conflict of interest.

Funding

This research was funded by the INTER program and co-funded by the Fond National de la Recherche, Luxembourg (FNR) and the Fund for Scientific Research-FNRS, Belgium (F.R.S—FNRS), T.0233.20—'Sustainable Residential Densification' project (SusDens, 2020–2024).

Data availability

The code supporting this study, comprising the scenario simulation engine, analysis and spatial metrics workflows, is openly available as the SuSceMod Python package on https://doi.org/10.5281/zenodo.15163673, with source code available at https://github.com/Anachak355/SuSceMod. Illustrative examples for both BAU and GAU scenario modelling are provided as Jupyter notebooks with example rasters in the repository. The MNL coefficients used for scenario simulation are provided in Table S2 (see supplementary material). The independent variables used in this study are publicly accessible from the sources listed in Table 1: road and railway data from OpenStreetMap, elevation and slope data from the Geoportal of Wallonia (https://geoportail.wallonie.be), and population and employment data from Statbel (https://statbel.fgov.be). The cadastral data used to derive the built-up density maps are sourced from the Belgian Land Registry and are subject to data access conditions; interested researchers may contact the corresponding author for further information.

Acknowledgements

The author(s) would like to express their gratitude to Prabhath Chilakalapudi from the Max Planck Institute of Sustainable Materials, Düsseldorf, for their valuable assistance in coding and the development of the Python package used in this research.

References

Al-Ahmadi, K., See, L., Heppenstall, A., Hogg, J., 2009. Calibration of a fuzzy cellular automata model of urban dynamics in Saudi Arabia. Ecological Complexity 6, 80–101. doi:10.1016/J.ECOCOM.2008.09.004.

Barros, C.P., Balsas, C.J.L., 2020. Luanda's Slums: An overview based on poverty and gentrification. Urban Development Issues 64, 29–38. doi:10.2478/UDI-2019-0021.

Batty, M., 1997. Cellular Automata and Urban Form: A Primer. Journal of the American Planning Association 63, 266–274. doi:10.1080/01944369708975918.

C. Montgomery, D., A. Peck, E., Vining, G.G., 2012. Transformation and weighting to correct model inadequacies, in: Introduction to linear regression analysis. 5th ed.. John Wiley & Sons, Inc.. chapter 5, pp. 171–187. doi:10.1111/insr.12020_10.

Cammerer, H., Thieken, A.H., Verburg, P.H., 2013. Spatio-temporal dynamics in the flood exposure due to land use changes in the Alpine Lech Valley in Tyrol (Austria). Natural Hazards 68, 1243–1270. doi:10.1007/S11069-012-0280-8.

Chakraborty, A., Joshi, M.Y., Mustafa, A., Cools, M., Teller, J., 2025. Model's parameter sensitivity assessment and their impact on Urban Densification using regression analysis. Geography and Sustainability 6, 100276. doi:10.1016/J.GEOSUS.2025.100276.

Chakraborty, A., Mustafa, A., Omrani, H., Teller, J., 2023. A Framework to Probe Uncertainties in Urban Cellular Automata Modelling Using a Novel Framework of Multilevel Density Approach: A Case Study for Wallonia Region, Belgium. Urban Book Series Part F270, 325–341. doi:10.1007/978-3-031-31746-0_17.

Chakraborty, A., Mustafa, A., Teller, J., 2024a. City Planning Dynamics: A Theoretical Framework of Urban Development Scenario of Belgium Provinces Using Logit Based Cellular Automata, in: GEOProcessing 2024 : The Sixteenth International Conference on Advanced Geographic Information Systems, Applications, and Services, IARIA, Barcelona, Spain. pp. 14–17. URL: https://www.thinkmind.org/library/GEOProcessing/GEOProcessing_2024/geoprocessing_2024_1_40_30039.html.

Chakraborty, A., Mustafa, A., Teller, J., 2024b. Modelling multi-density urban expansion using Cellular Automata for Brussels Metropolitan Development Area. ISPRS Annals of the Photogrammetry, Remote Sensing and Spatial Information Sciences X-4/W4-2024, 29–34. doi:10.5194/ISPRS-ANNALS-X-4-W4-2024-29-2024.

Chakraborty, A., Omrani, H., Teller, J., 2022a. A Comparative Analysis of Drivers Impacting Urban Densification for Cross Regional Scenarios in Brussels Metropolitan Area. Land 2022, Vol. 11, Page 2291 11, 2291. doi:10.3390/LAND11122291.

Chakraborty, A., Omrani, H., Teller, J., 2022b. Modelling the Drivers of Urban Densification to Evaluate Built-up Areas Extension: A Data-Modelling Solution Towards Zero Net Land Take. Lecture Notes in Computer Science (including subseries Lecture Notes in Artificial Intelligence and Lecture Notes in Bioinformatics) 13376 LNCS, 260–270. doi:10.1007/978-3-031-10450-3_21.

Charliers Julien, Reginster Isabelle, 2024. Artificialization of soil, urban sprawl and land availability: where is Wallonia? - Iweps. URL: https://www.iweps.be/wp-content/uploads/2024/09/RS12-Territoire.pdf.

Chen, Y., Li, X., Liu, X., Ai, B., 2014. Modeling urban land-use dynamics in a fast developing city using the modified logistic cellular automaton with a patch-based simulation strategy. International Journal of Geographical Information Science 28, 234–255. doi:10.1080/13658816.2013.831868.

Claassens, J., Koomen, E., Rouwendal, J., 2020. Urban density and spatial planning: The unforeseen impacts of dutch devolution. PLOS ONE 15, e0240738. doi:10.1371/journal.pone.0240738.

Clarke, K.C., Hoppen, S., Gaydos, L.J., 1996. Methods and techniques for rigorous calibration of a cellular automaton model of urban growth, in: Third International Conference/Workshop on Integrating GIS and Environmental Modeling, National Center for Geographic Information and Analysis, Santa Fe, New Mexico. pp. 1319–1328. URL: https://pubs.usgs.gov/publication/70202456.

Colsaet, A., Laurans, Y., Levrel, H., 2018. What drives land take and urban land expansion? A systematic review. Land Use Policy 79, 339–349. doi:10.1016/J.LANDUSEPOL.2018.08.017.

Congalton, R.G., 1991. A review of assessing the accuracy of classifications of remotely sensed data. Remote Sensing of Environment 37, 35–46. doi:10.1016/0034-4257(91)90048-B.

CPDT, 2024. Territorial development plan, Belgium. URL: https://territoire.wallonie.be/storage/territoire/documents/content/page/wallonie-2050/analyse-contextuelle-.pdf.

Dewan, A.M., Yamaguchi, Y., 2009. Land use and land cover change in Greater Dhaka, Bangladesh: Using remote sensing to promote sustainable urbanization. Applied Geography 29, 390–401. doi:10.1016/J.APGEOG.2008.12.005.

ESPON, 2020. Territorial patterns and relations in Belgium - Country fiche | ESPON. URL: https://archive.espon.eu/belgium.

Esposito, P., Patriarca, F., Salvati, L., 2018. Tertiarization and land use change: The case of Italy. Economic Modelling 71, 80–86. doi:10.1016/J.ECONMOD.2017.12.002.

European Commission, 2021. EU Soil Strategy for 2030: Reaping the benefits of healthy soils for people, food, nature and climate. Technical Report COM(2021) 699 final. European Commission. Brussels. URL: https://eur-lex.europa.eu/legal-content/EN/TXT/?uri=celex:52021DC0699.

Hanocq, P., 2011. Territorial planning system and urban development - From a deterministic to a strategic model. 7th International Conference on Virtual Cities and Territories , 319–325URL: https://hdl.handle.net/2268/112982.

Hu, Z., Lo, C.P., 2007. Modeling urban growth in Atlanta using logistic regression. Computers, Environment and Urban Systems 31, 667–688. doi:10.1016/J.COMPENVURBSYS.2006.11.001.

Kasanko, M., Barredo, J.I., Lavalle, C., McCormick, N., Demicheli, L., Sagris, V., Brezger, A., 2006. Are European cities becoming dispersed?: A comparative analysis of 15 European urban areas. Landscape and Urban Planning 77, 111–130. doi:10.1016/J.LANDURBPLAN.2005.02.003.

Li, X., Yeh, A.G.O., 2000. Modelling sustainable urban development by the integration of constrained cellular automata and GIS. International Journal of Geographical Information Science 14, 131–152. doi:10.1080/136588100240886.

Liu, Y., Li, L., Chen, L., Cheng, L., Zhou, X., Cui, Y., Li, H., Liu, W., 2019. Urban growth simulation in different scenarios using the SLEUTH model: A case study of Hefei, East China. PLOS ONE 14, e0224998. doi:10.1371/JOURNAL.PONE.0224998.

Mustafa, A., Bruwier, M., Archambeau, P., Erpicum, S., Pirotton, M., Dewals, B., Teller, J., 2018a. Effects of spatial planning on future flood risks in urban environments. Journal of Environmental Management 225, 193–204. doi:10.1016/J.JENVMAN.2018.07.090.

Mustafa, A., Heppenstall, A., Omrani, H., Saadi, I., Cools, M., Teller, J., 2018b. Modelling built-up expansion and densification with multinomial logistic regression, cellular automata and genetic algorithm. Computers, Environment and Urban Systems 67, 147–156. doi:10.1016/J.COMPENVURBSYS.2017.09.009.

Mustafa, A., Saadi, I., Cools, M., Teller, J., 2018c. Understanding urban development types and drivers in Wallonia: A multi-density approach. International Journal of Business Intelligence and Data Mining 13, 309–330. doi:10.1504/IJBIDM.2018.088434.

Mustafa, A., Van Rompaey, A., Cools, M., Saadi, I., Teller, J., 2018d. Addressing the determinants of built-up expansion and densification processes at the regional scale. Urban Studies 55, 3279–3298. doi:10.1177/0042098017749176.

Naikoo, M.W., Shahfahad, Talukdar, S., Ishtiaq, M., Rahman, A., 2023. Modelling built-up land expansion probability using the integrated fuzzy logic and coupling coordination degree model. Journal of Environmental Management 325, 116441. doi:10.1016/J.JENVMAN.2022.116441.

OpenStreetMap Foundation contributors, 2024. OpenStreetMap. URL: https://www.openstreetmap.org/#map=8/50.510/4.475.

Overmars, K.P., De Koning, G.H., Veldkamp, A., 2003. Spatial autocorrelation in multi-scale land use models. Ecological Modelling 164, 257–270. doi:10.1016/S0304-3800(03)00070-X.

Poelmans, L., Van Rompaey, A., 2009. Detecting and modelling spatial patterns of urban sprawl in highly fragmented areas: A case study in the Flanders–Brussels region. Landscape and Urban Planning 93, 10–19. doi:10.1016/J.LANDURBPLAN.2009.05.018.

Poelmans, L., Van Rompaey, A., 2010. Complexity and performance of urban expansion models. Computers, Environment and Urban Systems 34, 17–27. doi:10.1016/j.compenvurbsys.2009.06.001.

Pontius, G.R., Schneider, L.C., 2001. Land-cover change model validation by an ROC method for the Ipswich watershed, Massachusetts, USA. Agriculture, Ecosystems & Environment 85, 239–248. doi:10.1016/S0167-8809(01)00187-6.

Public service of Wallonia, 2020. Téléchargement des données | Géoportail de la Wallonie. URL: https://geoportail.wallonie.be.

Rwanga, S.S., Ndambuki, J.M., Rwanga, S.S., Ndambuki, J.M., 2017. Accuracy Assessment of Land Use/Land Cover Classification Using Remote Sensing and GIS. International Journal of Geosciences 8, 611–622. doi:10.4236/IJG.2017.84033.

Seto, K.C., Fragkias, M., Güneralp, B., Reilly, M.K., 2011. A Meta-Analysis of Global Urban Land Expansion. PLoS ONE 6, e23777. doi:10.1371/JOURNAL.PONE.0023777.

SPW, 2017. Report on the state of the Walloon environment 2017 - State of the Walloon environment. Technical Report. Service public de Wallonie;Département de l'étude du milieu naturel et agricole;DGO3 - Direction générale des ressources naturelles, de l'agriculture et de l'environnement. URL: https://etat.environnement.wallonie.be/contents/publications/rapport-sur-letat-de-lenvironnement-wallon-2017.html.

Statbel, 2017. About Statbel | Statbel. URL: https://statbel.fgov.be/en/about-statbel.

Thorne, J.H., Santos, M.J., Bjorkman, J.H., 2013. Regional Assessment of Urban Impacts on Landcover and Open Space Finds a Smart Urban Growth Policy Performs Little Better than Business as Usual. PLOS ONE 8, e65258. doi:10.1371/JOURNAL.PONE.0065258.

Ullah, Ibrar, 2022. Re-identifying the Rural/Urban: A case Study of Pakistan. Espaço e Economia 11. doi:10.4000/ESPACOECONOMIA.22019.

Vermeiren, K., Van Rompaey, A., Loopmans, M., Serwajja, E., Mukwaya, P., 2012. Urban growth of Kampala, Uganda: Pattern analysis and scenario development. Landscape and Urban Planning 106, 199–206. doi:10.1016/J.LANDURBPLAN.2012.03.006.

Wang, Y.P., Kintrea, K., 2021. Urban Expansion and Land Use Changes in Asia and Africa. Environment and Urbanization ASIA 12, S13–S17. doi:10.1177/0975425321999081.

White, R., Engelen, G., 1997. Cellular Automata as the Basis of Integrated Dynamic Regional Modelling. Environment and Planning B 24, 235–246. doi:10.1068/B240235.

White, R., Engelen, G., 2000. High-resolution integrated modelling of the spatial dynamics of urban and regional systems. Computers, Environment and Urban Systems 24, 383–400. doi:10.1016/S0198-9715(00)00012-0.

Zhang, B., Wang, H., 2021. A new type of dual-scale neighborhood based on vectorization for cellular automata models. GIScience and Remote Sensing 58, 386–404. doi:10.1080/15481603.2021.1883946.

Supplementary Material

Land take futures under divergent urban growth scenarios: Cellular automata-based stress-testing for No Net Land Take targets

---

S1 Demand Calculation and Extrapolation

Table S1: Class to class transition of urban built-up demand (with percentages).

Years		Class 0	Class 1	Class 2	Class 3
2000–2010	Class 0	1,391,031	*7169 (27.60%)	*5247 (20.20%)	*1271 (4.89%)
	Class 1		70,983	†7920 (30.50%)	†248 (0.95%)
	Class 2			149,554	†4115 (15.85%)
	Class 3				52,582
2010–2020	Class 0	1,381,843	*4906 (26.28%)	*3538 (18.95%)	*744 (3.99%)
	Class 1		72,337	†5613 (30.07%)	†202 (1.08%)
	Class 2			159,056	†3665 (19.63%)
	Class 3				58,216

* Expansion, † Densification

S1.1 Worked example: BAU and GAU demand extrapolation

We use an example to illustrate the demand extrapolation equations (Eqs. 1a-1b in the main text) further. We observe a demand of 7169 cells from class 0 to 1 for the years 2000–2010 (detailed transition figures in Table S1). We first calculate the change rate to be

$$d = \frac{D_{2020} - D_{2010}}{2020 - 2010} = \frac{490.6 - 716.9\,(hectare/year)}{2020 - 2010\,(years)} = -22.63\,ha/year^2$$

A decline in yearly demand for any class transition is hence characterised by a negative change rate. Similarly, we have calculated the demand for the remaining class transitions of reference class 0 to 2 and 3, reference class 1 to 2 and 3, and reference class 2 to 3. The change rate is now used to calculate the demand for any year after n (after 2020, in our case). We get, for instance, the demand in the year 2030 to be

$$\begin{aligned} D_{2030} = D_{2020} + (2030 - 2020) \times d &= 490.6 + 10 \times (-22.63) \\ &= 264.3\,ha/year \text{ or } 0.72\,ha/day \end{aligned}$$

We thus see the demand for urban expansion decrease over time.

Coming to the case of GAU, we assume a constant demand for every year after year n (2020, in our case), and hence the change rate d to be 0. The demand in the year 2030 and the subsequent years, for the GAU case, from class 0 to 1 transition would hence be

$$D_{2030} = D_{2020} = 490.6\, ha/year \text{ or } 1.34\, ha/day$$

which is higher than the value in the BAU scenario. Similarly, in both cases, demands are calculated for the remaining class transitions. This example, thus, clearly demonstrates how the trend varies in each case – a linear extrapolation in the BAU scenario, while being a constant demand in the GAU scenario.

S2 Multinomial Logistic Regression Model

S2.1 Full model specification

The probability maps are obtained for each class by the following equation

$$\begin{aligned} \log(k_1) &= \alpha_{k_1} + \beta_{k_1\mathrm{DEM}}\,(\mathrm{DEM}) + \beta_{k_1\mathrm{SL}}\,(\mathrm{SL}) + \cdots + \beta_{k_1\mathrm{ZON}}\,(\mathrm{ZON}) \\ &\vdots \\ \log(k_n) &= \alpha_{k_n} + \beta_{k_n\mathrm{DEM}}\,(\mathrm{DEM}) + \beta_{k_n\mathrm{SL}}\,(\mathrm{SL}) + \cdots + \beta_{k_n\mathrm{ZON}}\,(\mathrm{ZON}) \end{aligned} \tag{S1}$$

where $k_1, \ldots, k_n$ denote the built-up density classes considered in each transition, and DEM, SL, ..., ZON are the independent variables listed in Table 1 of the main text.

S2.2 Calibration results

Table S2: MNL coefficients for variables across class to class transitions for the years 2000-2010

Name	Abbreviation	Coefficients for Class to Class Transitions					
		0 to 1	0 to 2	0 to 3	1 to 2	1 to 3	2 to 3
Elevation	DEM	0.042	-0.016	*-0.152	*0.098	-0.032	-0.060
Slope	SL	*-0.091	*-0.428	*-1.119	*-0.149	*-0.725	*-0.503
Distance to Road 1	ER1	-0.013	*-0.174	*-0.831	*-0.079	-0.266	*-0.214
Distance to Road 2	ER2	0.020	*-0.106	*-0.403	-0.036	*-0.292	*-0.134
Distance to Road 3	ER3	*-0.147	*-0.255	*-0.279	-0.008	*-0.369	*-0.090
Distance to Road 4	ER4	*-0.361	*-0.317	-0.113	-0.031	-0.226	*-0.127
Distance to Railway Stations	ERS	0.043	0.028	*-0.262	0.027	0.031	-0.038
Distance to Large Sized Cities	ELC	*-0.036	0.001	*0.216	0.038	0.117	*0.074
Distance to Medium Sized Cities	EMC	-0.007	-0.027	0.045	*-0.065	-0.147	-0.033
Employment Density	EMD	*-0.114	0.050	*0.171	*-0.057	*0.177	*0.144
Population	POP	0.000	*0.000	*0.000	0.000	0.000	0.000
Zoning	ZON	*3.450	*3.035	*3.374	*2.193	*0.745	*0.657

*Variable is significant at a p-value < 0.01

Table S3: ROC value of MNL model for each density class transition (row to column).

	Class 1	Class 2	Class 3
Class 0	0.790	0.840	0.930
Class 1	–	0.989	0.991
Class 2	–	–	0.978

S3 Model Validation

S3.1 Formal definitions: ROC/AUC and Cohen's Kappa

The ROC curve measures the trade-off between the True Positive Rate (TPR) – the proportion of actual urban transitions correctly identified – and the False Positive Rate (FPR) – the proportion of non-urban cells incorrectly classified as urban, as defined below.

$$TPR = \frac{True\,Positives}{True\,Positives + False\,Negatives} \tag{S2a}$$

$$FPR = \frac{False\,Positives}{False\,Positives + True\,Negatives} \tag{S2b}$$

The AUC is calculated as

$$AUC = \int_0^1 TPR(x)\,dx \tag{S3}$$

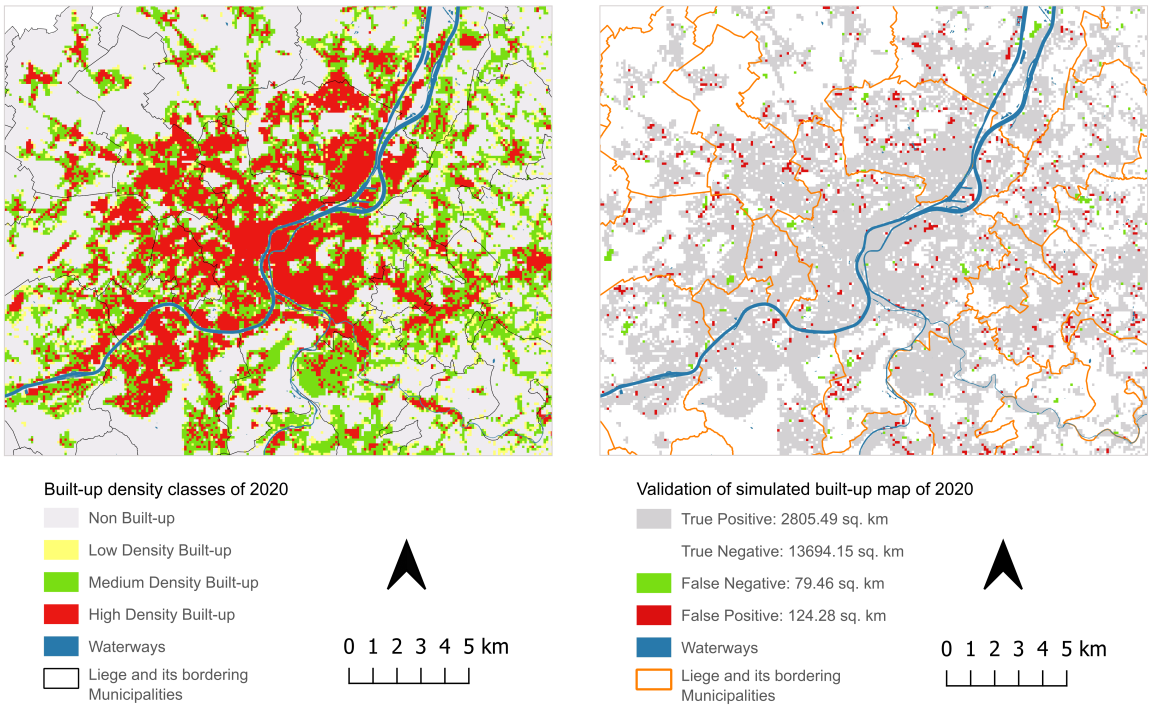
where TPR(x) is the True Positive Rate as a function of the threshold x, and dx represents the infinitesimal change in the False Positive Rate.

The general formula of Cohen's Kappa is expressed as

$$\kappa = \frac{P_o - P_e}{1 - P_e} \tag{S4}$$

where P_o is the observed agreement (accuracy) and P_e is the expected agreement by chance.

S3.2 Validation maps



(a) Zoomed image of Liège municipality showing built-up density classes for the year 2020

(b) Accuracy map, showing pixel-level comparison of urban growth model between observed and simulated map of 2020.

Figure S1: Validation of the MNL-CA model for the city of Liège and its surroundings, 2020.

S4 Future Scenario Projections

Table S4: Class-to-class demand for simulated urban built-up of 2030–2050 under the BAU and GAU scenarios.

Years		BAU				GAU			
		Class 0	Class 1	Class 2	Class 3	Class 0	Class 1	Class 2	Class 3
2020–2030	Class 0	1377173	2640	1820	210	1372673	4900	3530	740
	Class 1		73793	3300	150		71433	5610	200
	Class 2			164997	3210			164547	3660
	Class 3				62827				62827
2030–2040	Class 0	1376673	380	120	0	1363503	4900	3530	740
	Class 1		75333	990	110		70523	5610	200
	Class 2			167357	2760			170027	3660
	Class 3				66397				67427
2040–2050	Class 0	1376673	0	0	0	1354333	4900	3530	740
	Class 1		75653	0	60		69613	5610	200
	Class 2			166157	2310			175507	3660
	Class 3				69267				72027

Table S5: Projected urban growth across density classes (2020–2050) under BAU and GAU scenarios

		BAU Scenario			**GAU Scenario**		
Density Class	Area-2020	Area-2050	Change	Growth (%)	Area-2050	Change	Growth (%)
Class 0	1381707	1372819	-8888	-0.64	1354333	-27374	-1.98
Class 1	77679	75393	-2286	-2.94	74513	-3166	-4.08
Class 2	168057	169328	1271	0.76	184647	16590	9.87
Class 3	62704	72580	9876	15.75	76627	13923	22.20
Overall	308440	317301	8861	2.87	335787	27347	8.87

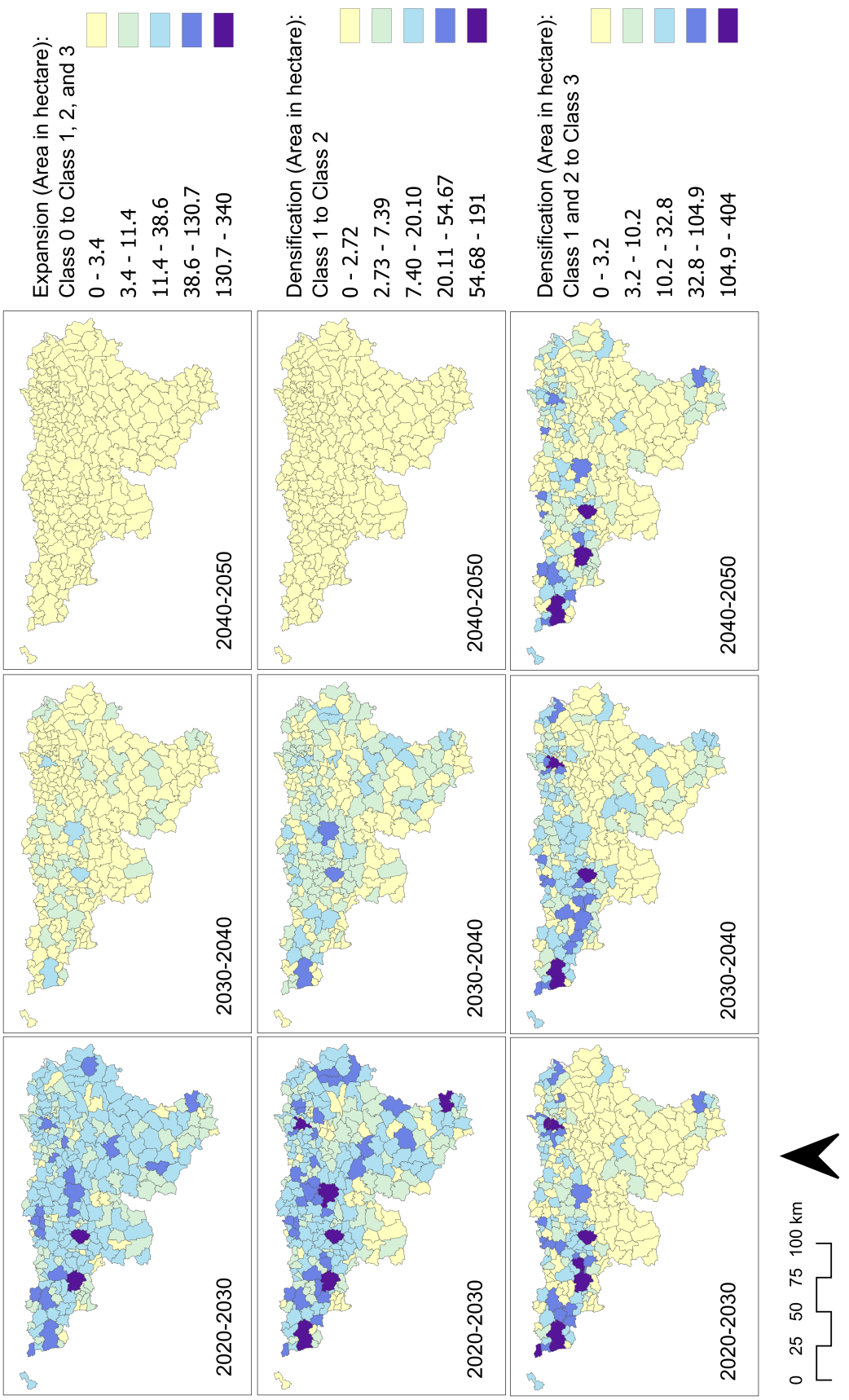


Figure S2: Choropleth maps showing total built-up area per municipality under the BAU scenario for 2020–2030, 2030–2040 and 2040–2050. Map lines delineate study areas and do not necessarily depict accepted national boundaries.

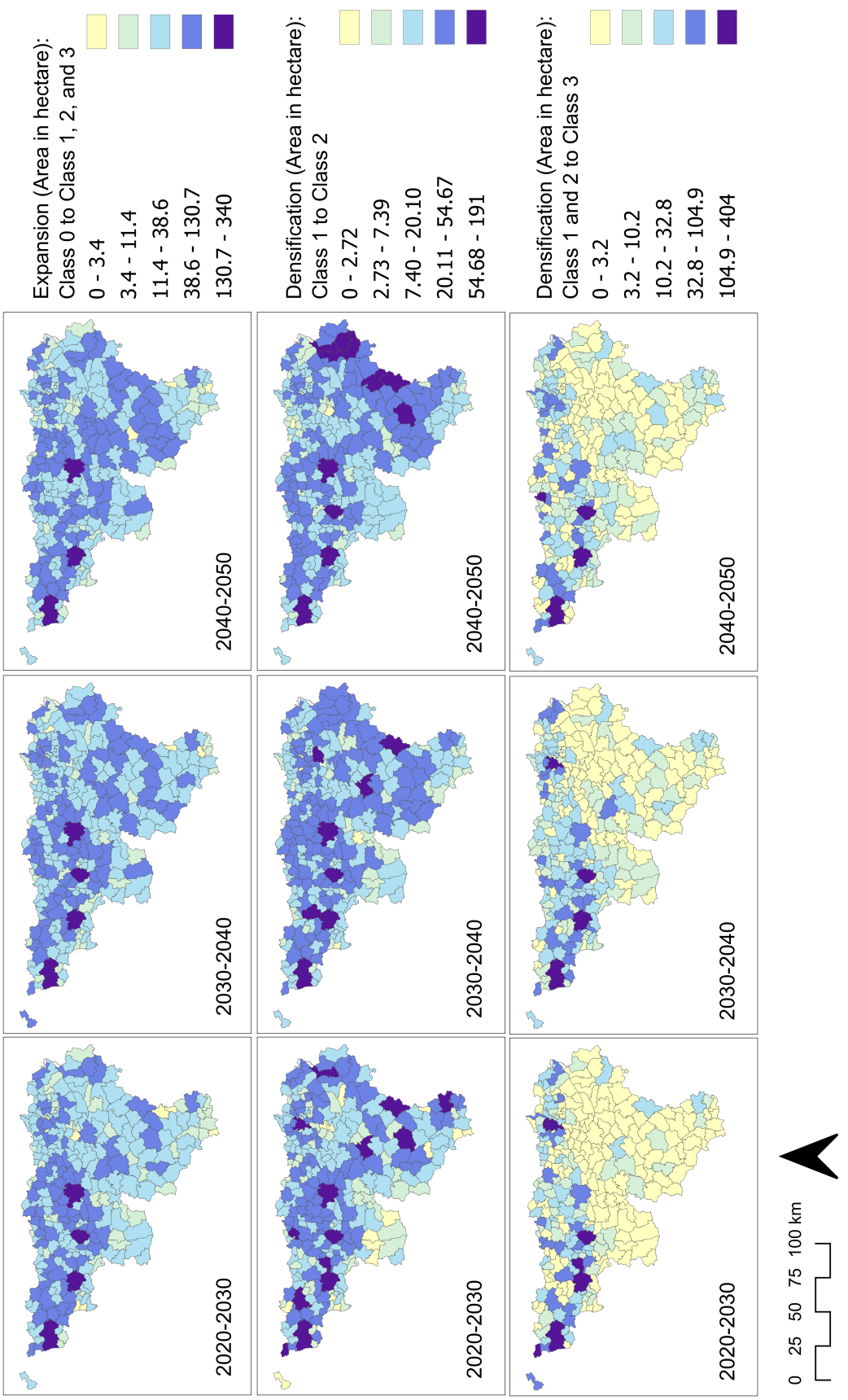


Figure S3: Choropleth maps showing total built-up area per municipality under the GAU scenario for 2020–2030, 2030–2040 and 2040–2050. Map lines delineate study areas and do not necessarily depict accepted national boundaries.